Progress in Oceanography 225 (2024) 103283

Contents lists available at ScienceDirect

Progress in Oceanography

journal homepage: www.elsevier.com/locate/pocean

A switch in thermal and haline contributions to stratification in the Greenland Sea during the last four decades

Caroline V.B. Gjelstrup *, Colin A. Stedmon

National Institute of Aquatic Resources, Technical University of Denmark, 2800 Lyngby, Denmark

ARTICLE INFO

Keywords:
Stratification
Temperature and salinity
Turner angle
Ocean convection
Sea-ice
Climate
Nordic Seas
Greenland Sea

ABSTRACT

Stratification and its thermal and haline contributions are important ocean properties of fundamental climatic influence. Upper-ocean stratification shapes marine ecosystems by regulating nutrient availability and deep-ocean stratification is important for carbon sequestration and ventilating the ocean interior. Here, we first assess the applicability of an ocean reanalysis product in representing stratification in the Nordic Seas and East Greenland Shelf. While the reanalysis performs well in most interior basins, it exhibits significant shortcomings on the East Greenland shelf, raising concerns about the reanalysis product in these areas. We then examine the development in the thermal and haline contributions to summer upper- (100 m) and winter intermediate- (1000 m) ocean stratification in the Greenland Sea from 1980 to 2020. We find that there has been a transition in the controls of winter stratification in the upper 1000 m of the Greenland Sea. The transition was associated with a westward migration of the boundary between salinity- and temperature-stratified waters and eventual switch from haline to thermal control of winter stratification. With that follows a change in the type of forcing that can lead to convection: The Greenland Sea is now less dependent on eroding salinity gradients but rather depends on cooling to overcome stratification. There has been a similar switch in summer stratification in the upper-ocean of the Greenland Sea where surface waters shifted from variable stratification, alternating between salinity and temperature dominance, to a stable temperature-stratified regime. This switch coincided with declining sea-ice concentrations related to the disappearance of the Odden ice tongue after 1997. The high sea-ice conditions previously characteristic of the Greenland Sea are now rare suggesting the transition will persist with potential implications for marine ecology and local sea-ice formation. Our findings reveal differences in how thermal and haline stratification has developed over the last 40 years, which may help explain or predict plankton production and carbon uptake and export.

1. Introduction

Stratification is an essential ocean property due to its role in regulating climate, ocean biogeochemical cycles and marine food webs (IPCC, 2019). Changes in stratification can have widespread consequences, as it impacts the coupling between surface and subsurface waters affecting the exchange of carbon, nutrients and oxygen between surface and deep layers. This, in turn, impacts carbon sequestration in the deep, and nutrient availability in the upper-ocean. Uncertainties surrounding how stratification in the Arctic region will respond to a warming climate and accelerated hydrological cycle has invoked speculation on future productivity (ultimately the distribution and magnitude of fisheries and the biological carbon pump) and the future intensity of deep ocean convection (Bhatt et al., 2014; Heuzé et al., 2022; Randelhoff and Guthrie, 2016; Slagstad et al., 2015). For example, there remains an ambiguity in how water column stratification will respond to reduced sea ice coverage. On the one hand, an increased sea-ice derived meltwater flux would strengthen upper-ocean stratification. On the other hand, some regions may experience a smaller influence of sea-ice meltwater as the sea-ice edge continues to retreat, which in combination with greater exposure to the atmosphere and winds, would decrease stratification. Recent studies report evidence to support both scenarios. In the Fram Strait, meltwater from sea-ice was shown to enhance stratification (Tuerena et al., 2021; von Appen et al., 2021) and von Appen et al. (2021) further suggest that this could become commonplace in the Arctic as the seasonal sea-ice zone broadens. In contrast, Våge et al. (2018) and Moore et al. (2022) show increased oceanic heat fluxes following sea-ice retreat along the East Greenland

* Corresponding author.
E-mail address: cvbgj@aqua.dtu.dk (C.V.B. Gjelstrup).

https://doi.org/10.1016/j.pocean.2024.103283
Received 31 August 2022; Received in revised form 29 October 2023; Accepted 17 May 2024
Available online 22 May 2024

continental slope implying weaker stratification and deeper mixed layers. These opposing effects emphasize the need for a spatially explicit assessment of changing stratification.

Not only is the strength of stratification crucial, but its relative contributions from temperature and salinity is of foremost importance to the functioning of the region (Carmack, 2007). For instance, open ocean sea-ice can only form where a strong halocline prevents thermal convection. Furthermore, the nature of upper ocean stratification affects air-sea exchange of heat, freshwater, CO_2 amongst other tracers, and hereby also shapes the structure of marine food webs (Carmack, 2007 and references therein). Recognition of the fundamental differences between regions stratified by temperature and salinity motivated categorisation of oceanic waters into alpha (α) and beta (β) type oceans (Carmack and Wassmann, 2006). Whilst α- and β-oceans are permanently stratified by temperature and salinity, respectively, the transition zones that lie in between either have equal contributions from temperature and salinity or are intermittently stratified by either property (Stewart and Haine, 2016). This ocean-type generally exhibits weak stratification and is therefore conducive to vertical exchange of water properties (Carmack, 2007).

The Nordic Seas host all three ocean-types. The Norwegian and Lofoten basins in the east are α-type oceans reflecting the warm and saline Atlantic Origin Waters (AtOW) that occupy the upper 400–600 m (Jeansson et al., 2017; Latarius and Quadfasel, 2016). These waters originate from the subtropical North Atlantic and are brought northwards across the Greenland-Scotland Ridge with two branches of the Norwegian Atlantic Current (Fig. 1). The temperature and salinity in this layer is above 3 °C and 34.95, respectively. This part of the Nordic Seas has been called the Atlantic domain (Swift and Aagaard, 1981). A salinity minimum denotes the cooler intermediate layer below consisting of Norwegian Sea Arctic Intermediate Water (NSAIW) with salinities between 34.87 and 34.90 and densities between 1027.97 kg m^{-3} and 1028.06 kg m^{-3} (Jeansson et al., 2017). NSAIW is supplied by advection of various intermediate waters including those formed convectively in the Greenland and Iceland Seas (Jeansson et al., 2017).

Cold, fresh Arctic Ocean outflow strongly influences the broad East Greenland Shelf imposing β-conditions in the western part of the Nordic Seas, corresponding to the area Swift and Aagaard (1981) refer to as the Polar domain. Here, Polar Water and denser intermediate waters formed or transformed within the central Arctic Ocean are brought southwards with the upper 150–200 m of the East Greenland Current (EGC; Aagaard and Coachman, 1968). The EGC also contains AtOW that has recirculated in Fram Strait and is identified as a temperature and salinity maximum (de Steur et al., 2014; Rudels et al., 2002).

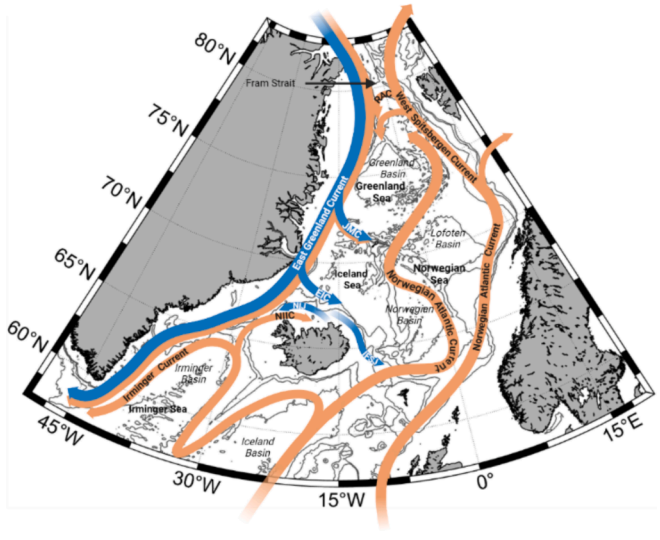

Fig. 1. Schematic of major circulation features in the Subpolar North Atlantic and Nordic Seas. Orange arrows represent warm, saline currents transporting transformed Atlantic Waters. Blue arrows represent comparatively cold and fresh waters of Polar and Arctic origin. RAC: Return Atlantic Current, NIIC: North Icelandic Irminger Current, NIJ: North Icelandic Jet, IFSJ: Iceland-Faroe Slope Jet, JMC: Jan Mayen Current, EIC: East Iceland Current. Created with BioRender.com.

A sharp salinity gradient separates the Polar domain from the interior Greenland and Iceland Seas, which comprise the Arctic domain. Eddies and eastward flowing currents facilitate exchange between the boundary currents and these interior basins (Blindheim and Østerhus, 2005). For instance, the Jan Mayen Current and East Icelandic Current (Fig. 1) transport low salinity waters from the EGC into the southern parts of the Greenland and Iceland Seas, respectively. Similarly, the Return Atlantic Current (RAC) brings AtOW across Fram Strait to merge with the EGC from where it subsequently enters the Greenland Sea (Hattermann et al., 2016).

The vertical structure in the Greenland Sea is regularly eroded by winter convection. Large horizontal gradients of temperature and salinity across the α/β fronts make the Greenland Sea particularly conducive to densification via cabbeling, upon mixing of two water masses with different thermohaline properties but similar densities due to the non-linear nature of the equation of state (Carmack, 2007). This creates a surface density maximum and stability minimum which are characteristic features of transition zones (Carmack, 2007; Stewart and Haine, 2016). In concert with sustained gyre circulation prolonging exposure to the atmosphere and strong heat loss in the Greenland Sea, these processes explain why the Greenland Sea is a key site of convection and deep-water formation (Stewart and Haine, 2016). The interior Greenland Sea is therefore unsurprisingly comprised of locally formed waters (Aagaard et al., 1985; Brakstad et al., 2019). These include the cold and very dense (>1030.444 kg m^{-3}) Greenland Sea Deep Water (GSDW) produced during deep-reaching convection. GSDW has, however, not been renewed since the late 1970's (Karstensen et al., 2005; Schlosser et al., 1991). Convection has only been observed to depths of 2000 m since then, producing the slightly warmer and less dense (>1027.97 kg m^{-3}) Greenland Sea Arctic Intermediate Water (GSAIW; Rudels et al., 2005; Brakstad et al., 2019).

The Nordic Seas have experienced extensive hydrographic changes over the past few decades (Smedsrud et al., 2022). The surface temperature has warmed at more than twice the rate of the global average (Rantanen et al., 2022; Saes et al., 2022) and loss of sea- and glacial-ice has enhanced the supply of freshwater to the upper-ocean (Solomon et al., 2021). Concurrent changes in the strength and composition of the Atlantic Water inflow across the Greenland-Scotland Ridge have altered the properties of the intermediate and deep layers (e.g. Glessmer et al., 2014; Lauvset et al., 2018; Mork et al., 2019; Tsubouchi et al., 2021). These ongoing hydrographic changes may alter the function of the region via changes in the strength of stratification and alterations to the locally dominant stratifying property. Understanding trends in stratification and its constituents is essential for assessing the Nordic Seas response to climatic change and provides a framework for assessing subsequent ecosystem impacts.

The aim of this study was to characterise water column stratification in the Nordic Seas and quantify changes in the horizontal distribution of its thermal and haline contributions in light of identifying the physical processes responsible. We hypothesise that although temperature and salinity changes can be density compensating, their relative importance has changed and this will not be uniform across the region. To this end, we take advantage of a state-of-the-art ocean reanalysis product providing continuous fields of temperature and salinity, allowing us to bridge the gap between in-situ observations and the spatio-temporal scales necessary for a spatially explicit assessment of regional stratification.

2. Data and methods

2.1. Reanalysis data

Continuous data fields were obtained from the Ocean Reanalysis System 5 (ORAS5) produced by the European Centre for Medium-range Weather Forecasts (ECMWF). The ORAS5 is an eddy-permitting ocean state reconstruction based on the NEMO 3.4.1 ocean model and forced with atmospheric fields from ERA-Interim for the 1979–2015 modelling period and ECMWF operational forecasts thereafter (Zuo et al., 2019). The product is constrained by observational data assimilated from the Met Office Hadley Centre EN4. ORAS5 provides monthly mean potential temperature and practical salinity fields on a 0.25° × 0.25° horizontal grid and at 75 depth levels with 1 m vertical resolution at the surface increasing to 200 m at depth (Zuo et al., 2019). The data product also includes monthly sea-ice concentration fields with the same spatial resolution.

2.2. Observational data

In-situ observations were used to assess the performance of ORAS5 in the Nordic Seas and adjacent shelf waters. To this end, temperature and salinity profiles collected by the global Argo program between 2001 and 2020 were downloaded (https://www.coriolis.eu.org/Data-Products/Data-selection, May 2022). Only "delayed mode" profiles that had undergone quality control and have adjusted values for temperature, salinity and pressure were used. A total of 73,248 profiles were available. These data were equally distributed across the year but biased towards the most recent decade and certain geographic areas (Fig. 2).

Very few Argo profiles are available from the shallow East Greenland shelf. To evaluate ORAS5 performance for this region we use two hydrographic data sets consisting of in-situ observations. The first is a compilation of bottle, CTD, expendable CTD and Argo float data from various sources published in Gjelstrup et al. (2022). The second consists of four hydrographic CTD sections sampled at approximately 60°N collected as part of the Overturning in the Subpolar North Atlantic Program (OSNAP; Pickart, 2018a; Pickart, 2018b; Pickart and McRaven, 2022a; Pickart and McRaven, 2022b). The sections were sampled in August or September in the years 2014, 2016, 2018 and 2020. Data were downloaded from https://www.o-snap.org/data-access/, October 2023.

2.3. Stratification criteria

Stratification is assessed as available potential energy (*APE*), which represents the work required to erode vertical density gradients and fully mix a water column down to a given depth. *APE* can be considered a bulk measure of stratification as it is an integral indicator of density variations in the water column. *APE* is given for each vertical profile by:

$$APE = \frac{1}{z_2 - z_1}\int_{z_2}^{z_1} gz\widehat{\rho}\ dz;\quad \widehat{\rho} = \rho(z) - \rho_{z_2} \tag{1}$$

Where, z_1 and z_2 are the depths between which *APE* is evaluated, g is gravitational acceleration, z is depth measured positively upwards from z_2 and ρ and ρ_{z_2} are density and density at z_2, respectively. Note, the integrand is scaled by 1 over layer thickness to arrive at units of energy per unit volume (J m^{-3}). Similar diagnostics have been called potential energy anomaly or simply potential energy (Simpson, 1981; Yamaguchi and Suga, 2019). Here, we follow the definition given in Polyakov et al., (2018) and use the name "*APE*" where the term "available" reflects the difference in energy between the observed state and a hypothetical state where the water column has uniform density.

2.3.1. Thermal and haline contributions toAPE

As density is primarily determined by temperature and salinity, the contribution of each to *APE* can be derived. Mathematically, the equation of state (EOS) expresses how temperature and salinity influence density. However, the complexity of the EOS makes it difficult to apply and a simplified EOS (S-EOS) formulated by Madec (2008) is used instead. In the S-EOS, density anomalies ($\Delta\rho$) from reference density are a function of temperature, salinity, and depth and it additionally accounts for the non-linear effects of cabbeling and thermobaricity:

$$\Delta\rho(T,S,z) = (-\alpha_0(1+0.5\lambda_1 T_V + \mu_1 z)T_V + \beta_0(1-0.5\lambda_2 S_V - \mu_2 z)S_V - \nu T_V S_V)/\rho_0 \tag{2}$$

Equation terms and values are given in Table 1. Ignoring the last cabbeling term, which is small across variable ranges relevant to this study (Appendix A), the thermal ($\Delta\rho_T$) and haline ($\Delta\rho_S$) contributions to the density anomaly are as follows:

$$\Delta\rho \cong \Delta\rho_T + \Delta\rho_S \tag{3}$$

$$\Delta\rho_T = (-\alpha_0(1+0.5\lambda_1 T_V + \mu_1 z)T_V)/\rho_0 \tag{4}$$

$$\Delta\rho_S = (\beta_0(1-0.5\lambda_2 S_V - \mu_2 z)S_V)/\rho_0 \tag{5}$$

Substituting equations (4) and (5) into (1), the thermal and haline contributions to *APE* are:

$$APE \cong APE' = APE_T + APE_S \tag{6}$$

$$APE_T = \frac{1}{z_2 - z_1}\int_{z_2}^{z_1} gz\widehat{\rho_T}\ dz;\quad \widehat{\rho_T} = \rho_T(z) - \rho_{Tz_2} \tag{7}$$

$$APE_S = \frac{1}{z_2 - z_1}\int_{z_2}^{z_1} gz\widehat{\rho_S}\ dz;\quad \widehat{\rho_S} = \rho_S(z) - \rho_{Sz_2} \tag{8}$$

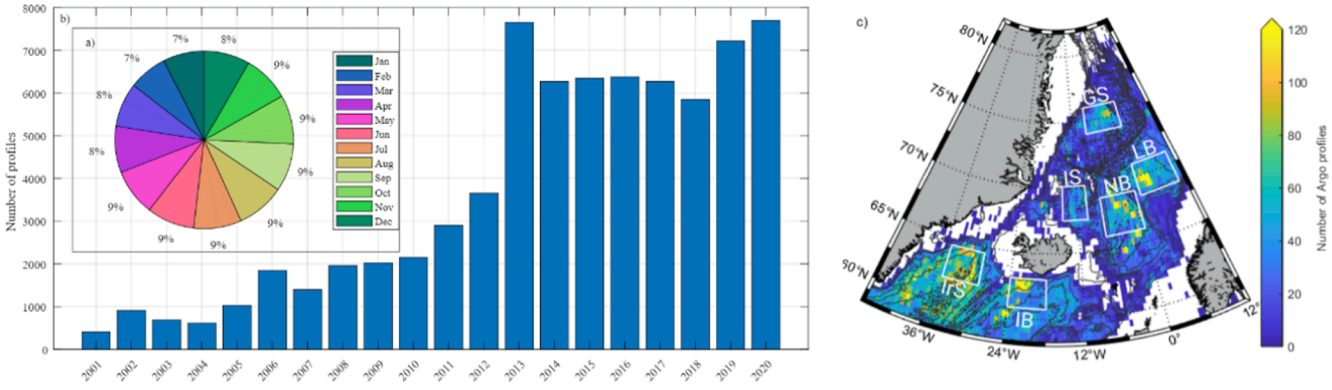

Fig. 2. Distribution of the Argo dataset by (a) month, (b) year and (c) region. The white polygons on (c) show the six areas used for the comparison, GS: Greenland Sea, LB: Lofoten Basin, NB: Norwegian Basin, IS: Iceland Sea, IrS: Irminger Sea and IB: Iceland Basin.

Table 1
Parameters and variables in (2).

Parameters/ variables	Description	Value	Units
α_0	Linear thermal expansion coefficient	$1.6550 \cdot 10^{-1}$	1/°C
β_0	Linear haline contraction coefficient	$7.6554 \cdot 10^{-1}$	kg/g
λ_1	Cabbeling coefficient in T^2	$5.9520 \cdot 10^{-2}$	$1/°C^2$
λ_2	Cabbeling coefficient in S^2	$5.4914 \cdot 10^{-4}$	$1/(g/kg)^2$
ν	Cabbeling coefficient in TS	$2.4341 \cdot 10^{-3}$	kg m^{-3} $°C^{-1}$ $(g/kg)^{-1}$
μ_1	Thermobaric coefficient in T	$1.4970 \cdot 10^{-4}$	1/(°C m)
μ_2	Thermobaric coefficient in S	$1.1090 \cdot 10^{-5}$	1/m
ρ_0	Reference density	1026	kg/m^3
T_V	$T - T_0$, where $T_0 = 10$ and T is temperature	–	°C
S_V	$S - S_0$, where $S_0 = 35$ and S is salinity	–	g/kg
z	Depth	–	m

Where the subscripts T and S refer to thermal and haline contributions, respectively.

2.3.2. Relative importance of thermal and haline contributions

The relative importance of the thermal and haline contributions can be gauged with the so-called Turner angle, *Ta*. Ruddick (1983) introduced the Turner angle as the four-quadrant arctangent of the ratio between the thermal and haline density contributions and it was originally used in studies of double diffusive mixing (You, 2002; Meccia et al., 2016). The metric has since been employed to identify drivers of density changes (Johnson et al., 2012) and define α- and β-ocean domains (Stewart and Haine, 2016). Here, the same concept is applied to derive a modified Turner angle weighting the relative importance of the thermal and haline contributions to *APE*:

$$Ta = \tan^{-1}(APE_T - APE_S\,,\, APE_T + APE_S) \quad (9)$$

Ta can in principle assume values between −180° and +180°, however, it is very unlikely for $|Ta| > 90°$ to occur as this represents statically unstable water column conditions (Fig. 3). In practice, *Ta* therefore ranges from −90° to +90°. Positive and negative *Ta* indicate thermal and haline dominance, respectively. Additionally, the thermal contribution is unstable for $-90° < Ta < -45°$ but compensated by salinity and vice versa for $45° < Ta < 90°$. The two contributions reinforce one another in the doubly stable range $-45° < Ta < 45°$ (Fig. 3). In Ruddick's original Turner angle, these intervals define waters conducive to double diffusive mixing. This rationale can, however, not be transferred to the modified Turner angle used in this study as our metric is based on an integral measure of water column stability. Conditions necessary to facilitate double diffusive mixing may therefore be present at specific depth levels but not when considering the water column in bulk.

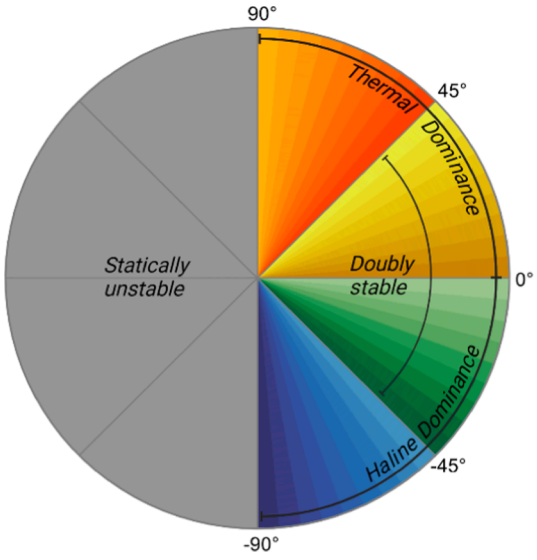

Fig. 3. Schematic of the modified Turner angle. Based on Ruddick (1983).

3. Results

3.1. Assessment of ORAS5 performance in the Nordic Seas

To assess whether the ORAS5 data product provides a reasonable ocean state estimate in the Nordic Seas, we compare it with the Argo dataset, which represents the most comprehensive collection of hydrographic measurements in this region. Because the Argo data set is assimilated in the construction of the ORAS5 itself, the comparison cannot be regarded as an independent validation, but rather an evaluation of how well the reanalysis product performs in the Nordic Seas. The comparison focuses on the six regions with best data availability: the Greenland Sea, Iceland Sea, Norwegian Basin, Lofoten Basin, Irminger Sea and Iceland Basin (Fig. 2).

ORAS5 performance is evaluated by comparing monthly mean temperature and salinity at 10 m, 100 m, 250 m, 500 m and 1000 m. Fig. 4 shows that ORAS5 reliably reproduces observed temperature and salinity ranges and variability across all tested depth levels. Discrepancies between the two data sets are generally small, although greater offsets are seen at the 500 m depth level in Lofoten Basin, where temperature is underestimated in ORAS5.

Additionally, the ability of ORAS5 to represent stratification with *APE* was assessed by comparing *APE* derived from ORAS5 and Argo profiles. Fig. 5 shows the outcome of the month-by-month comparison over the upper (0–97 m) and intermediate (0–1045 m) depth ranges. The comparison indicates that ORAS5 is well suited to characterise stratification with *APE*, as attested by the very strong correspondence between the Argo and ORAS5 based estimates across both depth ranges and all regions (Fig. 5). The Lofoten Basin is, however, an exception as ORAS5 underestimates *APE* over the intermediate depth range, which is likely caused by the cold-bias in ORAS5 that was identified at 500 m depth (Fig. 4d).

3.1.1. Assessment of ORAS5 performance on the East Greenland Shelf

The ability of the reanalysis product to reflect hydrographic conditions in the interior Nordic Seas offers assurance of its reliability where the observations are sufficient to anchor the underlying model. However, under-sampled regions such as the East Greenland shelf, are much less constrained. Harsh conditions have rendered this shelf region notoriously sparse in data and sea-ice cover hinders assimilation of surface information from satellites for much of the year. Consequently, reanalysis estimates in this region are highly dependent on model configuration and parameterisation.

To assess the reliability of the reanalysis product over the Northeast Greenland shelf (NEGS), we construct time series of temperature and salinity averaged over the surface 0–20 m, and at the core of the Polar and Atlantic Water layers defined by the temperature minimum and maximum, respectively, and compare with observational time series presented in Gjelstrup et al. (2022).

ORAS5 has difficulty in reproducing the hydrography of the NEGS, as seen by the large disparities in both temperature and salinity when compared to observational data (Fig. 6). Surface temperature is an exception hereto, as ORAS5 is within the range of available observations and replicates temporal variability fairly well. However, below the

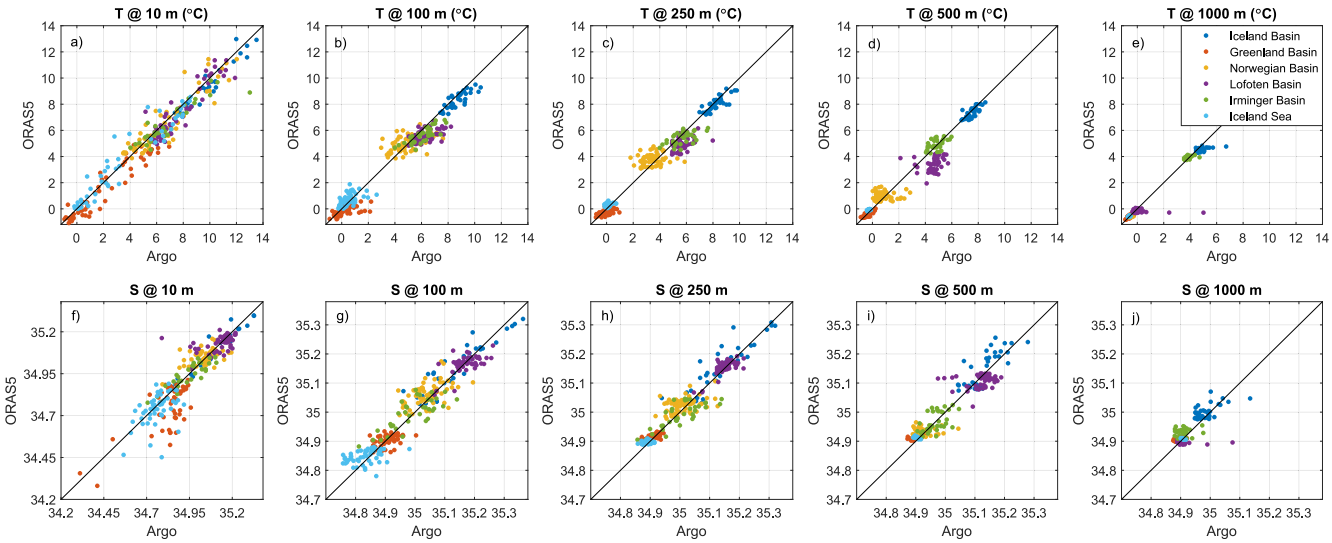

Fig. 4. Comparison of monthly mean temperature (a–e) and salinity (f–j) from Argo and ORAS5 at 10 m, 100 m, 250 m, 500 m and 1000 m in the six regions outline on Fig. 2.

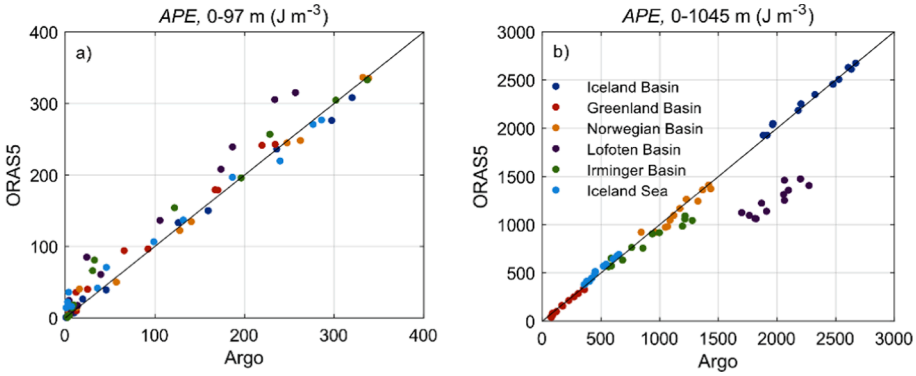

Fig. 5. Comparison of *APE* derived from ORAS5 and Argo dataset for *APE* calculated from the surface to 97 m (a) and 1045 m (b).

surface, there is a tendency for ORAS5 to overestimate temperature in the Polar Water layer and underestimate temperature in the Atlantic Water layer. Salinity discrepancies persist across all three layers considered. The discrepancies become particularly pronounced in recent years as the magnitudes of temporal changes are much weaker in ORAS5 compared to observations. This leads to salinity biases exceeding 1 unit of salinity in the last decade.

ORAS5 performance on the Southeast Greenland shelf (SEGS) is evaluated by comparing mean temperature and salinity sections across the OSNAP East line at approximately 60°N for summers when observations on the shelf are available, i.e. 2014, 2016, 2018 and 2020.

Despite many more available observations to anchor the reanalysis product on the SEGS compared to the NEGS, similar difficulties in accurately representing the shelf hydrography are evident (Fig. 7). The ORAS5 exhibits a warm bias over the shelf. The bias is largest at the surface (>2 °C) and decreases with depth to approximately 0.25 °C at 200 m (Fig. 7c). Salinity biases are similarly pervasive and most pronounced at the surface where differences between in-situ observations and the ORAS5 exceed 1.5 g kg^{-1} (Fig. 7f). This overestimation of salinity on the shelf results in a severe underestimation of the freshwater content (Fig. 8), suggesting an inaccurate or absent freshwater forcing in the models at this location.

The significant disparities between ORAS5 and actual temperature and salinity values can induce bias in stratification due to the non-linearity of the EOS. Because stratification is highly sensitive to temperature and salinity properties, these biases may induce misrepresentation of the actual stratification on the shelf. The remainder of this paper therefore focuses on the interior Nordic Seas where we have demonstrated that the ORAS5 provides a reliable representation of the hydrography.

3.2. Upper-ocean stratification

We investigate trends in upper-ocean stratification using *APE* calculated from the surface to 97 m depth, which is the nearest ORAS5 layer to 100 m. Over this depth range, *APE* is assumed to represent the stratification that will have greatest influence on nutrient and phytoplankton interactions in the photic zone and must be broken down to replenish surface waters with nutrients from below. We present results of the seasonal development of *APE* across the interior Nordic Seas and then focus on the Greenland Sea as the region with most pronounced interannual changes.

3.2.1. Seasonal development of APE

The upper-ocean stratification exhibits a strong seasonal cycle characterised by a single summer maximum and winter minimum (Fig. 9). All regions have a similar annual development with weakly stratified winters indicating a fully mixed upper 97 m of the water column. Stratification increases rapidly throughout the region in spring and reaches its peak in summer during August or September whereafter it gradually decays through autumn (Fig. 9d).

Annual development of the thermal contribution follows the sea-

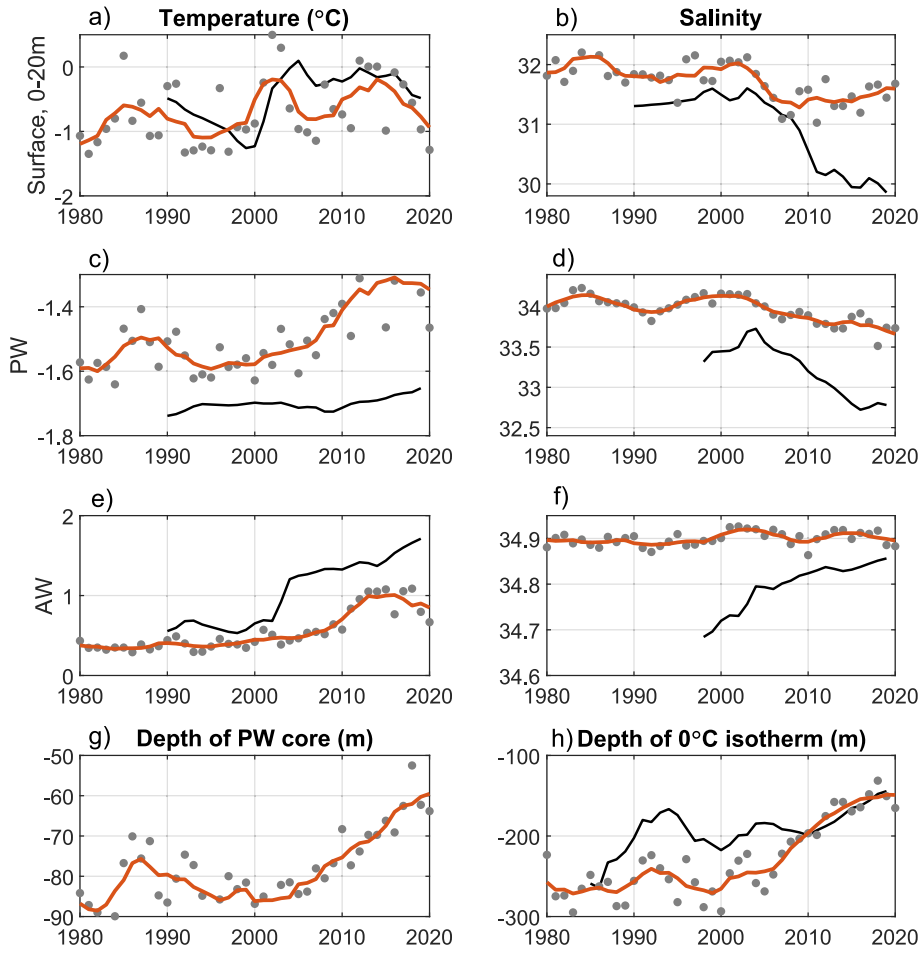

Fig. 6. Time series of temperature and salinity from ORAS5 and observations on the Northeast Greenland Shelf. Averaged over the surface 0–20 m (a & b), at the core of the Polar Water (PW) defined as the temperature minimum within the layer where $T < 0$ °C & $S < 34.4$ (c & d) and at the core of the Atlantic Water (AW) layer defined as the temperature maximum within the layer where $T > 0$ °C & $S > 34.4$. Panel (g) shows the vertical position of the Polar Water core and panel (h) shows the vertical position of the 0 °C isotherm. Grey circles are July-August-September averages and the orange line is a five-year running mean. Black lines show observational data reproduced from Gjelstrup et al. (2022).

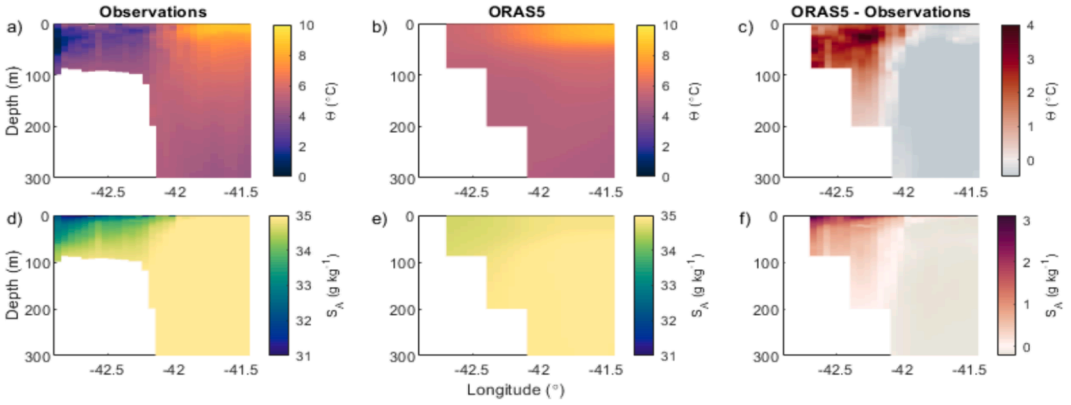

Fig. 7. Comparison of mean temperature (a & b) and salinity (d & e) sections across the shelf portion of the OSNAP East line between observations and the ORAS5 (a & c) reanalysis product (b & e). Panels (c) and (f) show the differences between observed and ORAS5 values in temperature and salinity, respectively.

sonal warming and cooling of the ocean surface (Fig. 9b and e). The magnitude of APE_T reflects the upper-ocean circulation pattern, with greatest values in the Norwegian and Irminger Seas that are dominated by Atlantic Water. Stratification is essentially only controlled by temperature in these regions. In contrast, the contributions from temperature and salinity are of similar magnitude in the Greenland Sea where temperatures are low year round and surface waters are influenced by freshwater from sea-ice melt and the EGC.

The narrow envelopes of standard deviation around the mean *APE* indicate that the magnitude of stratification has been relatively stable in all regions across the 1980–2020 period (Fig. 9d). However, variability particularly in salinity and APE_S in the Greenland Sea suggests a change

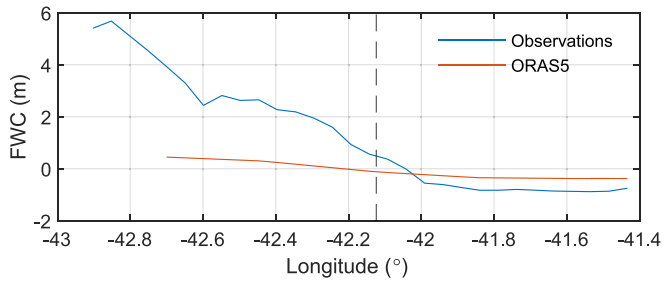

Fig. 8. Freshwater content (FWC; reference salinity 34.8) across the OSNAP East line averaged for 2014, 2016, 2018 and 2020 from observations (blue) and ORAS5 (orange). The stippled line indicates the 500 m isobath.

in the underlying temperature and salinity contributions in this region (Fig. 9 c and f).

3.2.2. *Temporal change in relative importance of temperature and salinity in the Greenland Sea*

Separating *APE* into its thermal and haline contributions further allows us to explore the evolution of upper-ocean stratification in the Greenland Sea. Fig. 10a reveals a clear transition from predominantly salinity-dominated stratification during the first half of the time series to predominantly temperature-dominated stratification during the second half of the time series on an annual basis. The transition was driven by an abrupt reduction in the haline contribution after 1997 (Fig. 10b). Prior to this, salinity dominated stratification for the majority of the year but large interannual fluctuations in APE_S caused the annual maximum *APE* to alternate between temperature- and salinity-dominated stratification (Fig. 10c). The modified Turner angle consequently assumed a broad range of values during summers reflecting the lack of a consistent dominant stratifying property in the first half of the time series (Fig. 10c).

After 1997, both the magnitude and interannual variability in APE_S was greatly reduced (Fig. 10b). This, in combination with a gradual increase in APE_T over the entire time series, caused a switch to temperature-dominated stratification during summers. A change point detection analysis confirms that this switch is a statistically robust feature (Two-sample T-test: p-value < 0.01). The switch was additionally associated with a significant reduction in the variability of the modified Turner angle before and after 1997 (σ^2 declined from 566 to 98; F-test for equality of variances: $p < 0.01$). The annual maximum stratification during the latter half of the time series is thus, consistently stratified by temperature (Fig. 10c).

The cessation of high APE_S years after 1997 coincides with a decline in winter sea-ice concentrations (Fig. 11). Correlation analysis reveals that more than 50 % of the variability in the annual maximum APE_S can be explained by the sea-ice concentration in the preceding winter (p-value < 0.01). Indeed, the probability density and spatial distributions of sea-ice concentration differ markedly before and after the regime shift in 1997. During the 1980–1997 period, the winter sea-ice concentration in the Greenland Sea was highly variable as indicated by the approximately flat probability density distribution (Fig. 11a). Some winters had little to no sea-ice cover over the interior Greenland Sea, whilst in other winters sea-ice extended northeastwards from the Jan Mayen Current into the interior Greenland Sea as a feature known as the Odden ice tongue (Fig. 11b). This feature appeared several times during the 1980–1997 period but was absent in all but two winters in the 1998–2020 period, where sea-ice concentrations were around 80 % (Fig. 11a). The changes in the distribution of sea-ice concentration together with the strong correlation with APE_S suggest that the switch in thermal and haline controls on stratification is tightly coupled to the disappearance of sea-ice.

3.3. *Winter intermediate-ocean stratification*

We now turn our attention to the intermediate-ocean stratification. The annual minimum *APE* is particularly interesting in this context as low (zero) *APE* indicates deep-reaching convection allowing for transfer of carbon and oxygen from the surface to the ocean interior. The following therefore focuses on the respective roles of heat and salt in

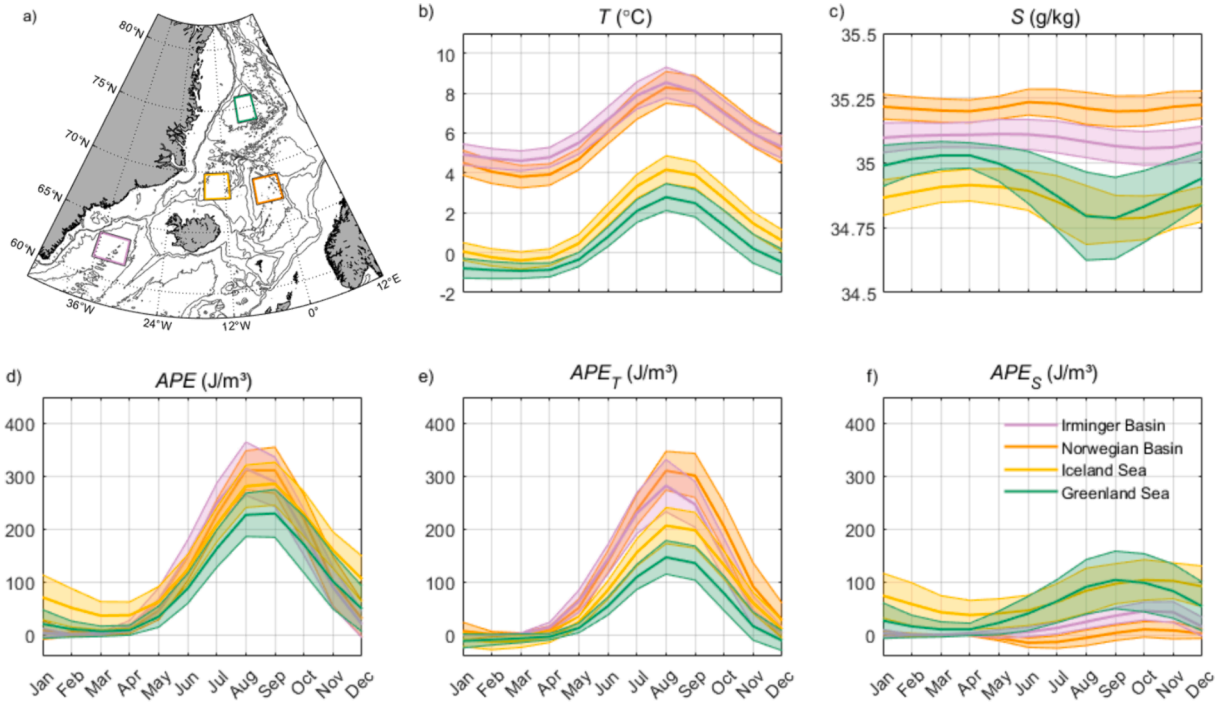

Fig. 9. Seasonal development of temperature, *T* (b), salinity, *S* (c), *APE* (d), APE_T (e) and APE_S (f) for the upper 97 m of the Greenland Sea (green), Iceland Sea (yellow), Norwegian Sea (orange) and Irminger Sea (purple). Thick lines indicate the mean over the 1980–2020 period and the shading indicates one standard deviation around the mean. The four regions are shown on panel (a).

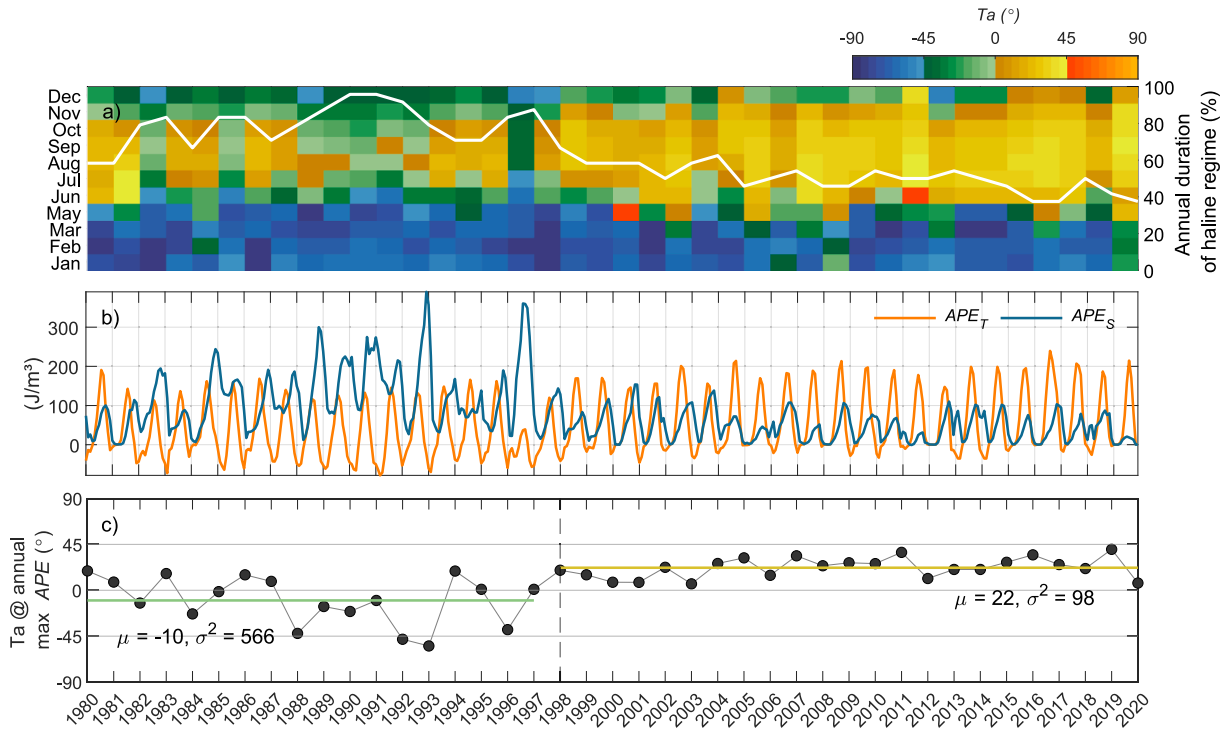

Fig. 10. Development in the thermal (APE_T) and haline (APE_S) contributions to upper-ocean stratification in the Greenland Sea as defined on Fig. 9a. Panel (a) shows the modified Turner angle for the Greenland Sea region as a Hovmöller diagram. The white line indicates the percentage of each year in which salinity stratification dominated ($Ta < 0°$). Panel (b) shows the time series of the thermal (APE_T) and haline (APE_S) contributions. Panel (c) shows the modified Turner angle at the annual maximum stratification (*APE*). The stippled vertical line denotes the 1998 regime shift and the horizontal lines give the regime-specific mean values.

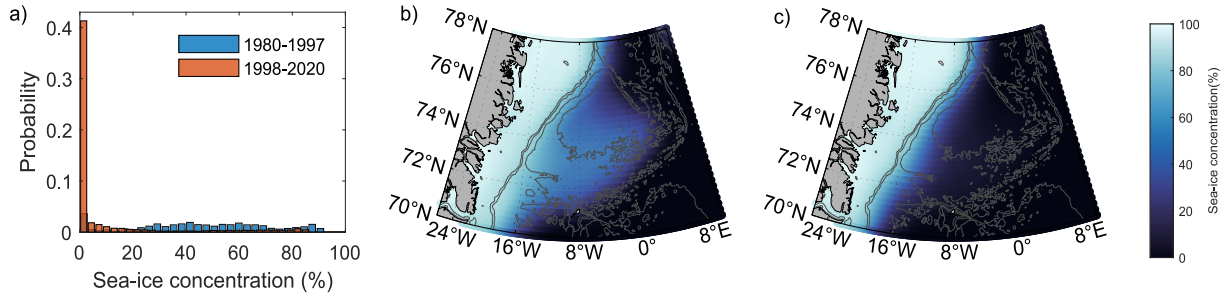

Fig. 11. Distribution of annual maximum sea-ice concentration before and after the regime shift identified in 1997. Panel (a) shows the frequency distribution for the two regimes in the Greenland Sea as defined on Fig. 9a. Panels (b) and (c) show the mean spatial distributions of sea-ice concentration before and after 1997, respectively. Bathymetry contours of −3000 m, −2000 m, −1000 m and −500 m are superimposed on panels (b) and (c).

determining the patterns and trends of annual minimum *APE* calculated from the surface to 1045 m. This depth was chosen based on Moore et al. (2015) who based on an idealised model estimate that mixed layers in key deep convection sites should seldom exceed 1000 m under typical atmospheric forcing in the 1979–2014 period.

3.3.1. Characteristics of the annual minimum APE

The annual minimum *APE* typically occurs in late winter after heat loss to the atmosphere, brine rejection and mechanical mixing have weakened vertical density gradients, and before summer warming and freshwater re-stratify the water column (Figs. 12a and 9c). The lowest *APE* minima are found in the Greenland Sea followed by western Irminger Sea. The same two regions experience the lowest variability in annual minimum *APE* (Fig. 12c). Correspondingly, linear regression analysis shows only modest rates of change in the magnitude of annual minimum *APE* (Fig. 12d).

3.3.2. Migration in thermal and haline contributions to annual minimum APE

The mean horizontal distribution of the modified Turner angle reflects the vertical structure of the water masses in the region. Strong thermal control is particularly obvious in the Iceland Basin and Norwegian Sea which are dominated by Atlantic Water (Fig. 13). These basins are characterised by high upper-ocean salinity and temperature due to the subtropical provenance of their source waters. In the Norwegian Sea, the less saline (but cold) NSAIW extends below as a salinity minimum causing an unstable vertical salinity gradient for which the vertical temperature gradient overcompensates ensuring overall stability. By contrast, the Greenland Sea and the western reaches of the Iceland Sea contain comparatively fresh waters with low temperatures such that the non-linearity of the EOS inherently lends itself to salinity-dominated stratification (Fig. 13).

The Greenland Sea and western Irminger Sea experience the greatest variability in terms of the relative importance of APE_T and APE_S for regulating winter stratification (Fig. 13b). These regions are doubly

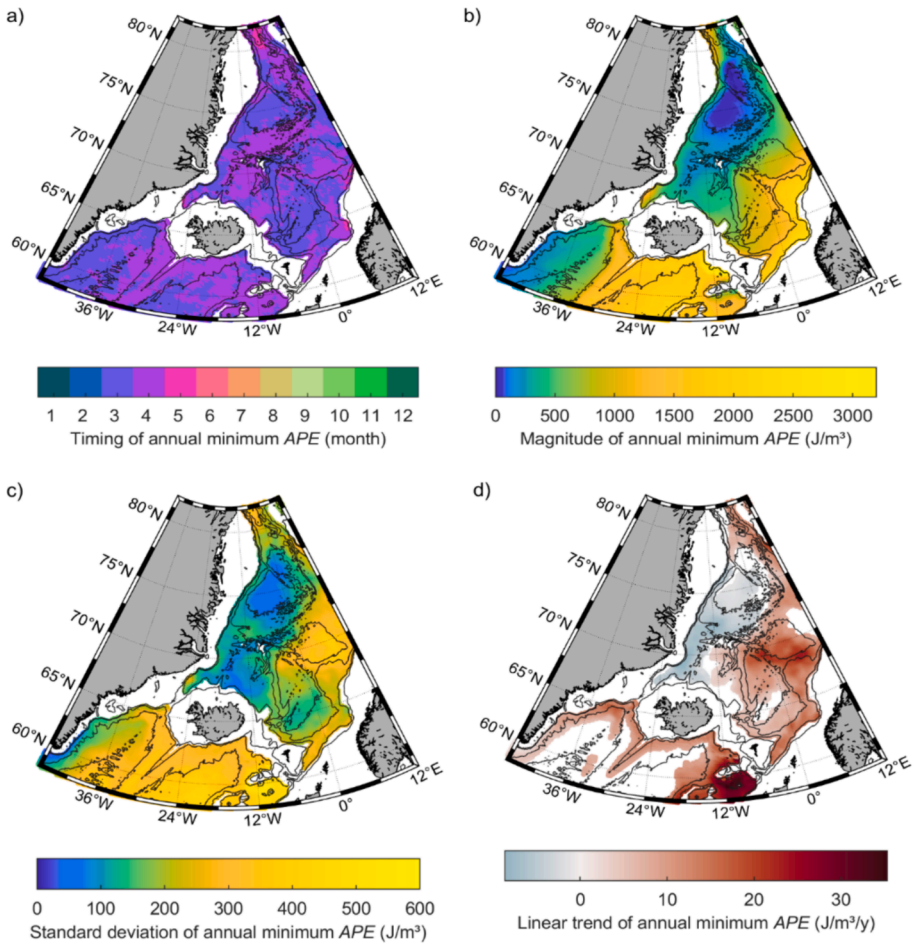

Fig. 12. Median timing (a), average magnitude (b) and standard deviation (c) of the annual minimum *APE*. Note non-linear colour scales on (b) and (c). The standard deviation was calculated over the entire forty-year period. Panel (d) shows statistically significant (p-value < 0.05) linear trends in annual minimum *APE* across the 1980–2020 period. Bathymetry contours of −3000 m, −2000 m, −1000 m and −500 m are superimposed on each panel.

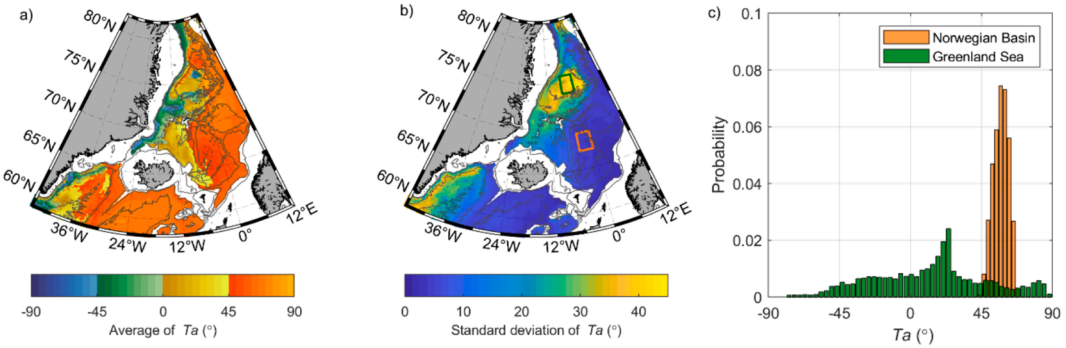

Fig. 13. Average (a) and standard deviation (b) of the relative importance of thermal and haline contributions to the annual minimum *APE* shown as the modified Turner angle. The standard deviation was calculated over the entire forty-year period. Panel (c) shows the probability density distribution of modified Turner angle within the Norwegian Sea (orange rectangle on (b)) and northern Greenland Sea (green rectangle on (b)) for the annual minimum *APE*.

stable ($-45° < Ta < 45°$) and are weakly stratified on average (Fig. 13a and 12b). Consequently, stratification is sensitive to small changes in temperature or salinity. Accordingly, the probability density distribution of the modified Turner angle from areas characterised by low *APE* is approximately flat (Fig. 13c). Conversely, areas of higher *APE* minima are characterised by high absolute modified Turner angles with a peaked probability density distribution (e.g. Norwegian Sea in Fig. 13c). There is, however, structure to the variability across the Greenland Sea. Fig. 14 shows the modified Turner angle at the timing of the annual minimum *APE* along a longitudinal transect crossing the Greenland and Norwegian Seas at 75°N. The relative importance of temperature and salinity changes gradually from haline dominance in the west (negative *Ta*) to thermal dominance in the east (positive *Ta*). The modified Turner angle gradually increases and stratification becomes thermally dominated between 1°E and 2°E as we enter the Norwegian Sea. In 1980–1989, salinity was the dominant stratifying property across the entire Greenland Sea. The relative importance of temperature increased drastically in the Greenland Sea over the subsequent three decades (Fig. 14),

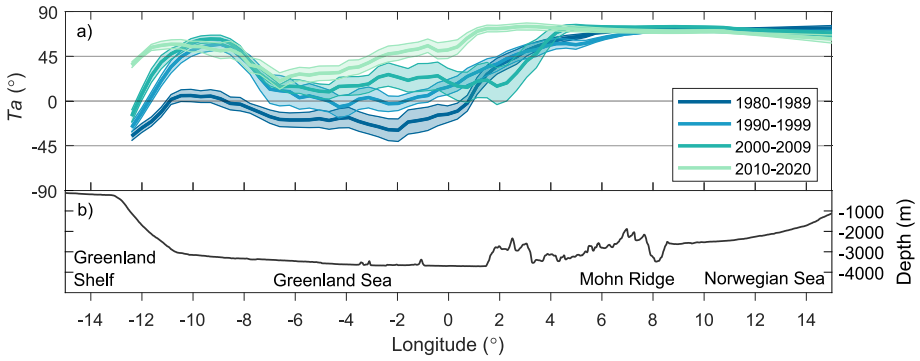

Fig. 14. Modified Turner angle (a) of annual minimum *APE* along a longitudinal transect at 75°N. The thick lines show decadal means and surrounding shading indicates one standard error. The colour bar on the right indicates the four stability regimes associated with the modified Turner angle. Panel (b) shows bathymetry along the same transect. Bathymetry from ETOPO1 (Amante and Eakins, 2009).

ultimately shifting the location of the transition from haline to thermal dominance westwards before the stretch of haline dominance was eroded entirely. This transition is not unique to the 75°N transect but reflects a basin-wide replacement of relatively cold, fresh salinity-stratified waters with warmer and more saline temperature-stratified waters. The latter spread southwestwards from the northern reaches of the Greenland Sea and along the RAC pathway eventually filling the majority of the basin (Fig. B1). The high variability in *Ta* is thus not simply because the Greenland Sea is a transition zone, but reflects a transition from predominantly salinity to temperature stratification over the intermediate depth range. Whilst this transition represents a large spatial change in the horizontal distribution of the dominant stratifying property, the strength of intermediate-ocean stratification has remained relatively stable. Hence, despite the fact that the water column exerts the same resistance to mechanical mixing as prior to the shift, a different mechanism is now needed to erode stratification and enable convection. A bulge between 8°W and 12°W is also apparent from Fig. 14. This feature is likely caused by the RAC which brings waters from the α-domain within the Nordic Seas across Fram Strait to return southwards with the EGC.

4. Discussion

4.1. Underperformance of the ORAS5 on the East Greenland shelf

In this paper, we use the ORAS5 reanalysis, a model-based product constrained by assimilated observations, to quantify changes in the controls of stratification in the Nordic Seas. An accurate representation of hydrography is an essential prerequisite for our study as the EOS can be highly sensitive to any temperature or salinity biases. We showed that ORAS5 reliably reproduces temperature and salinity properties throughout the water column in all deep basins, apart from the Lofoten Basin, when compared with Argo-based observations. However, we found significant shortcomings in ORAS5's representation of the East Greenland shelf hydrography, with substantial discrepancies in temperature and salinity compared to available observations. A prime example of this is the severe underestimation of freshwater content at 60°N suggesting that freshwater forcing in the underlying models is either inaccurate or altogether lacking at this location. The underperformance of the ORAS5 in this region underscores the complexities of modelling ocean dynamics on the shelf and in particular, the challenges related to the representation of freshwater forcing. Furthermore, the comparison highlights a need to re-evaluate how the assimilated data is weighted in the reanalysis, particularly in regions where the underlying models face known challenges.

The discrepancies and issues raised in this evaluation stress the importance of reconciling models and reanalyses with observational data for the East Greenland shelf. The scarce observational data from the region indicate that significant and rapid changes are taking place on the shelf and will continue (e.g. Karpouzoglou et al., 2022; Schaffer et al., 2017; Sejr et al., 2017). A refinement of the representation of connectivity between shelf and basin is of particular importance, especially concerning freshwater dynamics.

4.2. Regime shift in summer surface stratification in the Greenland Sea

Summer stratification in the upper water column of the Greenland Sea was shown to have undergone a regime shift in the relative contributions of temperature and salinity. A long-term increase in the thermal contribution was countered by an abrupt decrease in the haline contribution after 1997. These changes had no significant impact on the strength of upper-ocean stratification but caused a shift from predominantly salinity-dominated stratification to consistent temperature-dominated stratification during summers.

The abrupt decline in the haline contribution is particularly interesting in the context of the identified regime shift. The main sources of freshwater to the Greenland Sea are precipitation and lateral advection of freshwater from the EGC in either liquid or solid form. We do not consider change in precipitation and evaporation as plausible mechanisms for the abrupt decrease as studies suggest that precipitation and evaporation balance on seasonal timescales (Schmitt et al., 1989; Walsh and Portis, 1999). Two Great Salinity Anomaly events took place in the 1980's and 1990's suggesting that there may have been excess freshwater transport with the EGC during this period (Belkin, 2004). Diversion of this excess freshwater into the interior Greenland Sea could thus be a possible explanation for the strong haline contribution to stratification between 1980 and 1997. This period was additionally characterised by the occasional appearance of the Odden ice tongue which consisted of sea-ice advected from upstream regions and locally formed sea-ice (Wadhams and Comiso, 1999). The disappearance of the advected portion of this feature must therefore also have contributed to the decreased freshwater forcing in the second, temperature-dominated, regime. This was supported by a strong correlation (0.55) between the winter sea-ice concentration and the haline contribution the following summer.

In addition, the loss of sea-ice prolonged the exposure of the ocean surface to the atmosphere facilitating increased uptake of heat during summers. A recent study in the Fram Strait region demonstrated a strong relationship between the open water fraction and summer water temperatures at 55 m (de Steur et al., 2023). The same study additionally showed that summer insolation has extended the period of comparatively high upper-ocean temperatures until November, thereby altering the seasonal cycle. This provides an explanation for the prolonged annual duration of thermal stratification in the Greenland Sea.

The stark changes in the Greenland Sea represent a fundamental transition from summer stratification intermittently determined by

temperature or salinity, to consistent temperature-dominated stratification and has potential implications for regional marine ecology. For example, strong salinity stratification in the Greenland Sea during spring has been linked to high sea-ice export via Fram Strait and was further associated with early initiation of the annual phytoplankton bloom (Mayot et al., 2020). Under such conditions, the strong salinity stratification retains cells in the photic zone where the bloom rapidly develops until nutrients are exhausted. Based hereon, one may expect spring phytoplankton productivity to decrease in the Greenland Sea if the trend towards increased duration of thermal stratification continues into the spring months, which would dilute the phytoplankton biomass and delay the bloom. On the other hand, weaker upper-ocean stratification, as typically associated with α-oceans, increases the likelihood that wind driven mixing events can erode stratification and resupply nutrients during the productive period, ultimately inducing higher integrated primary production (Carmack and Wassmann, 2006). The shift towards a greater role of temperature in determining stratification may therefore entail a more gradual bloom development and an overall increase of the annual phytoplankton primary production, which in turn may increase export production and carbon sequestration.

4.3. Intermediate-depth winter convection in the Greenland Sea

Hydrographic variability in the intermediate layers stems from changes in winter convection and long-term trends. Variability in intermediate-ocean stratification was predominantly expressed as highly variable modified Turner angles concentrated in the Greenland Sea (Fig. 13b). Here, the thermal contribution to stratification increased steadily over the 1980–2020 period effectively shifting the α/β delineation westwards until thermally stratified waters prevailed across the entire Greenland Sea. These findings are consistent with extensive warming and salinification of the Greenland Sea gyre documented in previous studies (e.g. Latarius and Quadfasel, 2016; Lauvset et al., 2018; Brakstad et al., 2019). Analyses from Latarius and Quadfasel (2016) report increasing temperatures in the interior Greenland Sea across their 2001–2011 time period. A later study shows that this trend continued through to 2016 and was preceded by another period of warming in the intermediate layer from 1986 to 1995 (Lauvset et al., 2018). Salinity was highly variable until 2001 after which it increased throughout the water column but most intensely at 500 m (0.002 yr^{-1}) followed by 1000 m (0.001 yr^{-1}; Lauvset et al., 2018). Based on strong cross-correlations (0.72 for temperature and 0.8 for salinity) between surface anomalies in the Greenland Sea and Atlantic Water core properties at the Greenland-Scotland Ridge three years prior, the authors attribute these long-term trends to northward propagation of anomalies originating farther south. Most of the exchange between the Norwegian and the Greenland Seas is facilitated by the RAC as it brings AtOW to the EGC and is subsequently entrained into the Greenland Sea gyre (Håvik et al., 2017). A central role of the AtOW in driving the observed shift in density contributions fits well with the spatial pattern of the spreading of thermally stratified waters southwestwards along the RAC pathway (Fig. S1).

Despite the salinification that occurred in the early 2000's, a new less dense class of GSAIW documented by Brakstad et al. (2019) became the dominant water mass at intermediate depths following a period of reduced convective activity. The arrival of GSAIW initiated a new period of convective activity and consequently, the weakly stratified GSAIW occupied the entire intermediate depth range by the 2010's. The increased volume of weakly stratified waters has also reduced stability in the Greenland Sea. Herein lies an explanation for the slight negative trend in annual minimum *APE* identified on Fig. 12d. Thus, the shift in thermal and haline contributions to stratification is driven by a combination of local (convective) and remote (propagation of anomalies) processes.

Whilst the overall strength of stratification in the intermediate waters of the Greenland Sea have not changed considerably, the shift in thermal and haline contributions reveals that convection to 1000 m is now less dependent on eroding salinity gradients remnant from summer freshwater lenses. Instead, it now mainly depends on cooling, which appears sufficient despite the increasing temperatures of the waters entering the region. However, as Moore et al. (2015) showed a 20 % reduction in the magnitude of air-sea heat fluxes over the 1979–2010 period, winter cooling may not continue to suffice if the trend continues.

4.4. Is the Greenland Sea undergoing Atlantification?

Widespread oceanic changes fuelled by anomalous influx of warm, saline waters from the subarctic have been termed Atlantification in other Arctic regions (Ingvaldsen et al., 2021; Polyakov et al., 2017). Atlantification is typically associated with a weakening of stratification and increased heat supply from intermediate waters resulting in sea-ice loss (Polyakov et al., 2017).

The changes documented here in the Greenland Sea over both the upper- and intermediate-ocean depth ranges, may likewise be considered manifestations of Atlantification. We have shown a trend towards a greater role of AtOW in determining stratification over the intermediate depth range and further argue that this was related to the replacement of GSDW with GSAIW and associated with a slight decrease in the overall strength of winter stratification. Increased heat content of the upper-ocean and reduced freshwater forcing drove a switch to temperature-dominated stratification during summers and further prolonged the annual duration of thermal stratification. This is expected to alter primary production patterns to resemble those typical of α-oceans thereby suggesting possible ecological implications of the hydrographic changes.

Finally, the switch in thermal and haline controls on stratification over both depth ranges jointly pose a challenge for local sea-ice formation in the Greenland Sea. Due to the increase in upper-ocean temperature and surface salinification, the ocean must lose more heat than before in order to reach freezing temperature. Heat loss must also occur over a shorter period of time as suitable stratification conditions (haline stratification) have become less prevalent than before. The increased heat content and decreased stability of GSAIW compared to GSDW may further enhance the vertical heat flux potentially impeding the surface mixed layer from ever reaching freezing temperature. Thus, whilst sea-ice loss appears to be at least partially responsible for driving the regime shift in thermal and haline controls on upper-ocean stratification, the shift itself further implicates the potential for local sea-ice formation as the hydrographic conditions are less conducive to sea-ice formation than before the shift.

It is not possible to determine whether the switch in stratification contributed to the sea-ice decline based on the analysis presented here. However, it is clear that the observed changes have made it more challenging for sea-ice to form locally. The switch towards a greater role of temperature in determining stratification is therefore likely to persist. Surface stratification in the Greenland Sea is unlikely to return to the haline regime under current and future expected conditions, assuming Arctic freshwater is retained within the EGC. The hydrographic development of the Greenland Sea thus indicates that ongoing Atlantification of the Arctic region has also reached the Arctic domain of the Nordic Seas.

5. Summary and conclusion

In this study, we use the ORAS5 ocean reanalysis product to examine the development of stratification and its thermal and haline constituents over the upper (0–100 m) and intermediate (0–1000 m) depth ranges in the Nordic Seas. Comparison with available observations reveals both strengths and shortcomings in the ability of the reanalysis product to represent the hydrography of the Nordic Seas. While the reanalysis performs well in all interior basins apart from the Lofoten Basin, we find substantial deficiencies on the East Greenland shelf. These inadequacies cast doubt on the reliability of the product for these critical shelf regions,

emphasising the need for improved observational data and reanalysis techniques in such areas. Nevertheless, the comprehensive dataset afforded by the ORAS5 enables us to assess trends and variability in the interior basins over long time scales.

Analysis of the spatially and temporally continuous data fields showed modest changes in the strength of stratification across the majority of the Nordic Seas and both depth ranges despite extensive hydrographic changes. The relative importance of temperature and salinity has, however, changed and as a consequence, the horizontal distribution of temperature and salinity stratified waters has shifted.

This shift is exemplified in the intermediate winter waters in the Greenland Sea where relatively cold, fresh, salinity-stratified waters were replaced with warmer and more saline temperature-stratified waters over the 1980–2020 period. These events caused a progressive westward migration of the division between temperature- and salinity-stratified waters until the entire basin was thermally stratified by the 2010–2020 period. Whilst the switch had limited impact on the overall strength of stratification, convection is now reliant on surface heat loss rather than erosion of freshwater lenses to enable intermediate-depth convection.

A similar transition occurred in the summer surface waters in the Greenland Sea. Here, summer stratification transitioned from a highly variable regime, in which stratification was intermittently determined by either salinity or temperature, to a more stable regime characterised by consistent temperature-stratification. This switch coincided with a decline in sea-ice concentration, which in concert with sea-surface warming likely fuelled the transition. In addition to consistent temperature-dominated summer stratification, the annual duration of thermal dominance increased.

Jointly, the changes in stratification suggest that the Greenland Sea may be undergoing Atlantification with potential implications for local sea-ice formation and regional marine ecology.

Declaration of competing interest

The authors declare that they have no known competing financial interests or personal relationships that could have appeared to influence the work reported in this paper.

Data availability

The data used are freely available from Copernicus, Coriolis and OSNAP. Direct links are provided in the manuscript.

Acknowledgements

We thank the ECMWF for providing the ORAS5 dataset and all that have contributed with in-situ measurements, quality assurance, data delivery, assimilation and modelling. OSNAP data were collected and made freely available by the OSNAP (Overturning in the Subpolar North Atlantic Program) project and all the national programs that contribute to it (www.o-snap.org). This work was supported by the Technical University of Denmark and CAS acknowledges funding from the Independent Research Fund Denmark Grant No. 9040-00266B and the Nordic Council of Ministers AG-Fisk Grant number (209)-2020-LEGCO.

Appendix A. Supplementary material

Supplementary data to this article can be found online at https://doi.org/10.1016/j.pocean.2024.103283.

References

Aagaard, K., Coachman, L.K., 1968. The East Greenland Current north of Denmark Strait. Part I. ARCTIC 181–200. http://citeseerx.ist.psu.edu/viewdoc/summary?doi=10.1.1.490.2616.

Aagaard, K., Swift, J.H., Carmack, E.C., 1985. Thermohaline circulation in the Arctic Mediterranean Seas. J. Geophys. Res. 90 (C3), 4833. https://doi.org/10.1029/jc090ic03p04833.

Amante, C., Eakins, B.W., 2009. ETOPO1 global relief model converted to PanMap layer format. NOAA-National Geophysical Data Center, PANGAEA, accessed 1 February 2021. doi: 10.1594/PANGAEA.769615.

Belkin, I.M., 2004. Propagation of the "Great Salinity Anomaly" of the 1990s around the northern North Atlantic. Geophys. Res. Lett. 31 (8) https://doi.org/10.1029/2003GL019334.

Bhatt, U.S., Walker, D.A., Walsh, J.E., Carmack, E.C., Frey, K.E., Meier, W.N., Moore, S. E., Parmentier, F.J.W., Post, E., Romanovsky, V.E., Simpson, W.R., 2014. Implications of Arctic sea ice decline for the earth system. Annu. Rev. Env. Resour. 39, 57–89. https://doi.org/10.1146/ANNUREV-ENVIRON-122012-094357.

Blindheim, J., Østerhus, S., 2005. The Nordic Seas, main oceanographic features. In: The Nordic Seas: an Integrated Perspective: Oceanography, Climatology, Biogeochemistry, and Modeling. Wiley Blackwell, pp. 11–37. https://doi.org/10.1029/158GM03.

Brakstad, A., Våge, K., Håvik, L., Moore, G.W.K., 2019. Water mass transformation in the Greenland sea during the period 1986–2016. J. Phys. Oceanogr. 49 (1), 121–140. https://doi.org/10.1175/JPO-D-17-0273.1.

Carmack, E.C., 2007. The alpha/beta ocean distinction: a perspective on freshwater fluxes, convection, nutrients and productivity in high-latitude seas. Deep Sea Res. Part II 54 (23–26), 2578–2598. https://doi.org/10.1016/J.DSR2.2007.08.018.

Carmack, E., Wassmann, P., 2006. Food webs and physical-biological coupling on pan-Arctic shelves: unifying concepts and comprehensive perspectives. Prog. Oceanogr. 71 (2–4), 446–477. https://doi.org/10.1016/j.pocean.2006.10.004.

de Steur, L., Hansen, E., Mauritzen, C., Beszczynska-Möller, A., Fahrbach, E., 2014. Impact of recirculation on the East Greenland Current in Fram Strait: results from moored current meter measurements between 1997 and 2009. Deep Sea Res. Part 1 Oceanogr. Res. Pap. 92, 26–40. https://doi.org/10.1016/J.DSR.2014.05.018.

de Steur, L., Sumata, H., Divine, D.V., Granskog, M.A., Pavlova, O., 2023. Upper ocean warming and sea ice reduction in the East Greenland Current from 2003 to 2019. Commun. Earth Environ. 4 (1) https://doi.org/10.1038/s43247-023-00913-3.

Gjelstrup, C.V.B., Sejr, M.K., de Steur, L., Christiansen, J.S., Granskog, M.A., Koch, B.P., Møller, E.F., Winding, M.H.S., Stedmon, C.A., 2022. Vertical redistribution of principle water masses on the Northeast Greenland Shelf. Nat. Commun. 13 (12), 7660 https://doi.org/10.1038/s41467-022-35413-z.

Glessmer, M.S., Eldevik, T., Våge, K., Øie Nilsen, J.E., Behrens, E., 2014. Atlantic origin of observed and modelled freshwater anomalies in the Nordic Seas. Nat. Geosci. 7 (11), 801–805. https://doi.org/10.1038/ngeo2259.

Hattermann, T., Isachsen, P.E., Von Appen, W.J., Albretsen, J., Sundfjord, A., 2016. Eddy-driven recirculation of Atlantic Water in Fram Strait. Geophys. Res. Lett. 43 (7), 3406–3414. https://doi.org/10.1002/2016GL068323.

Håvik, L., Våge, K., Pickart, P.S., Harden, B., von Appen, W.-J., Jónsson, S., Østerhus, S., 2017. Structure and variability of the Shelfbreak East Greenland Current North of Denmark Strait. J. Phys. Oceanogr. 47 (10), 2631–2646. https://doi.org/10.1175/JPO-D-17-0062.1.

Heuzé, C., Mohrmann, M., Andersson, E., Crafoord, E., 2022. Global decline of deep water formation with increasing atmospheric CO2. Preprint Earth ArXiv. https://doi.org/10.31223/X56K6D.

Ingvaldsen, R.B., Assmann, K.M., Primicerio, R., Fossheim, M., Polyakov, I.V., Dolgov, A. V., 2021. Physical manifestations and ecological implications of Arctic Atlantification. Nat. Rev. Earth Environ. 2 (12), 874–889. https://doi.org/10.1038/s43017-021-00228-x.

IPCC, 2019. Summary for Policymakers. In: IPCC Special Report on the Ocean and Cryosphere in a Changing Climate [H.-O. Pörtner, D.C. Roberts, V. Masson-Delmotte, P. Zhai, M. Tignor, E. Poloczanska, K. Mintenbeck, A. Alegría, M. Nicolai, A. Okem, J. Petzold, B. Rama, N.M. Weyer (Eds.)]. Cambridge University Press, Cambridge, UK and New York, NY, USA, pp. 3–35. doi: 10.1017/9781009157964.001.

Jeansson, E., Olsen, A., Jutterström, S., 2017. Arctic Intermediate Water in the Nordic Seas, 1991–2009. Deep Sea Res. Part I 128, 82–97. https://doi.org/10.1016/J.DSR.2017.08.013.

Johnson, G., Schmidtko, S., Lyman, J., 2012. Relative contibutions of temperature and salinity to seasonal mixed layer density changes and horiztonal density gradients. J. Geophys. Res. Oceans 117 (C4). https://doi.org/10.1029/2011JC007651.

Karpouzoglou, T., de Steur, L., Smedsrud, L.H., Sumata, H., 2022. Observed changes in the Arctic Freshwater Outflow in Fram Strait. J. Geophys. Res. Oceans 127 (3), e2021JC018122. https://doi.org/10.1029/2021JC018122.

Karstensen, J., Schlosser, P., Wallace, D.W.R., Bullister, J.L., Blindheim, J., 2005. Water mass transformation in the Greenland Sea during the 1990s. J. Geophys. Res. Oceans 110 (7), 1–18. https://doi.org/10.1029/2004JC002510.

Latarius, K., Quadfasel, D., 2016. Water mass transformation in the deep basins of the Nordic Seas: analyses of heat and freshwater budgets. Deep Sea Res. Part I 114, 23–42. https://doi.org/10.1016/J.DSR.2016.04.012.

Lauvset, S.K., Brakstad, A., Våge, K., Olsen, A., Jeansson, E., Mork, K.A., 2018. Continued warming, salinification and oxygenation of the Greenland Sea gyre. Tellus A: Dyn. Meteorol. Oceanogr. 70 (1), 1–9. https://doi.org/10.1080/16000870.2018.1476434.

Madec, G., & the NEMO team, 2008. NEMO ocean engine. Note du Pôle de modélisation, Institut Pierre-Simon Laplace (IPSL), France, No 27, ISSN No 1288-1619.

Mayot, N., Matrai, P.A., Arjona, A., Bélanger, S., Marchese, C., Jaegler, T., Ardyna, M., Steele, M., 2020. Springtime export of arctic sea ice influences phytoplankton production in the Greenland Sea. J. Geophys. Res. Oceans 125 (3), e2019JC015799. https://doi.org/10.1029/2019JC015799.

Meccia, V.L., Simoncelli, S., Sparnocchia, S., 2016. Decadal variability of the Turner Angle in the Mediterranean Sea and its implications for double diffusion. Deep-Sea Res. I 114, 64–77. https://doi.org/10.1016/J.DSR.2016.04.001.

Moore, G.W.K., Våge, K., Pickart, R.S., Renfrew, I.A., 2015. Decreasing intensity of open-ocean convection in the Greenland and Iceland seas. Nat. Clim. Chang. 5 (9), 877–882. https://doi.org/10.1038/nclimate2688.

Moore, G.W.K., Våge, K., Renfrew, I.A., Pickart, R.S., 2022. Sea-ice retreat suggests re-organization of water mass transformation in the Nordic and Barents Seas. Nat. Commun. 13 (1), 1–8. https://doi.org/10.1038/s41467-021-27641-6.

Mork, K.A., Skagseth, Ø., Søiland, H., 2019. Recent warming and freshening of the Norwegian sea observed by Argo data. J. Clim. 32 (12), 3695–3705. https://doi.org/10.1175/JCLI-D-18-0591.1.

Pickart, R., 2018a. Conductivity-Temperature-Depth (CTD) data as part of the OSNAP (Overturning in the Subpolar North Atlantic Program), from 2014 on the R/V Knorr (KN221-03). Duke Digital Repository. https://doi.org/10.7924/r4qz26535.

Pickart, R., 2018b. Conductivity-Temperature-Depth (CTD) data as part of the OSNAP (Overturning in the Subpolar North Atlantic Program), from 2016 on the R/V Neil Armstrong. Duke Digital Repository. https://doi.org/10.7924/r4m61gc19.

Pickart, R., McRaven, R., 2022a. Conductivity-Temperature-Depth (CTD) data as part of the Overturning in the Subpolar North Atlantic Program (OSNAP), from 2018 on the R/V Neil Armstrong. Georgia Tech Digital Repository. https://doi.org/10.35090/gatech/66765.

Pickart, R., McRaven, R., 2022b. Conductivity-Temperature-Depth (CTD) data as part of the Overturning in the Subpolar North Atlantic Program (OSNAP), from 2020 on the R/V Neil Armstrong. Georgia Tech Digital Repository. https://doi.org/10.35090/gatech/66767.

Polyakov, I.V., Pnyushkov, A.V., Alkire, M.B., Ashik, I.M., Baumann, T.M., Carmack, E. C., Goszczko, I., Guthrie, J., Ivanov, V.V., Kanzow, T., Krishfield, R., Kwok, R., Sundfjord, A., Morison, J., Rember, R., Yulin, A., 2017. Greater role for Atlantic inflows on sea-ice loss in the Eurasian Basin of the Arctic Ocean. Science 356 (6335), 285–291.

Polyakov, I.V., Pnyushkov, A.V., Carmack, E.C., 2018. Stability of the arctic halocline: a new indicator of arctic climate change. Environ. Res. Lett. 13 (12), 125008.

Randelhoff, A., Guthrie, J.D., 2016. Regional patterns in current and future export production in the central Arctic Ocean quantified from nitrate fluxes. Geophys. Res. Lett. 43 (16), 8600–8608. https://doi.org/10.1002/2016GL070252.

Rantanen, M., Karpechko, A.Y., Lipponen, A., Nordling, K., Hyvärinen, O., Ruosteenoja, K., Vihma, T., Laaksonen, A., 2022. The Arctic has warmed nearly four times faster than the globe since 1979. Commun. Earth Environ. 3 (168) https://doi.org/10.1038/s43247-022-00498-3.

Ruddick, B., 1983. A practical indicator of the stability of the water column to double-diffusive activity. Deep-Sea Res. I 30, 1105–1107.

Rudels, B., Fahrbach, E., Meincke, J., Budéus, G., Eriksson, P., 2002. The East Greenland Current and its contribution to the Denmark Strait overflow. ICES J. Mar. Sci. 59 (6), 1133–1154. https://doi.org/10.1006/jmsc.2002.1284.

Rudels, B., Björk, G., Nilsson, J., Winsor, P., Lake, I., Nohr, C., 2005. The interaction between waters from the Arctic Ocean and the Nordic seas north of Fram Strait and along the East Greenland Current: Results from the Arctic Ocean-02 Oden expedition. J. Mar. Syst. 55 (1–2), 1–30. https://doi.org/10.1016/j.jmarsys.2004.06.008.

Saes, M.J.M., Gjelstrup, C.V.B., Visser, A.W., Stedmon, C.A., 2022. Separating annual, decadal and regional change in Sea Surface Temperature in the Northeastern Atlantic and Nordic Seas. J. Geophys. Res.: Oceans 127 (8), e2022JC018630. https://doi.org/10.1029/2022JC018630.

Schaffer, J., von Appen, W.-J., Dodd, P.A., Hofstede, C., Mayer, C., de Steur, L., Kanzow, T., 2017. Warm water pathways toward Nioghalvfjerdsfjorden Glacier, Northeast Greenland. J. Geophys. Res. Oceans 122 (5), 4004–4020. https://doi.org/10.1002/2016JC012462.

Schlosser, P., Bönisch, G., Rhein, M., Bayer, R., 1991. Reduction of deepwater formation in the Greenland Sea during the 1980s: evidence from tracer data. Science 251 (4997), 1054–1056. https://doi.org/10.1126/science.251.4997.1054.

Schmitt, R.W., Bogden, P.S., Dorman, C.E., 1989. Evaporation minus precipitation and density fluxes for the North Atlantic. J. Phys. Oceanogr. 19, 1208–1221.

Sejr, M.K., Stedmon, C.A., Bendtsen, J., Abermann, J., Juul-Pedersen, T., Mortensen, J., Rysgaard, S., 2017. Evidence of local and regional freshening of Northeast Greenland coastal waters. Sci. Rep. 7 (13183) https://doi.org/10.1038/s41598-017-10610-9.

Simpson, J.H., 1981. The shelf-sea fronts: implications of their existence and behaviour. Philos. Trans. R. Soc. Lond. Ser. A, Math. Phys. Sci. 302 (1472), 531–546. https://doi.org/10.1098/rsta.1981.0181.

Slagstad, D., Wassmann, P.F.J., Ellingsen, I., 2015. Physical constraints and productivity in the future Arctic Ocean. Front. Mar. Sci. 2 (OCT), 85 https://doi.org/10.3389/FMARS.2015.00085/BIBTEX.

Smedsrud, L.H., Muilwijk, M., Brakstad, A., Madonna, E., Lauvset, S.K., Spensberger, C., Born, A., Eldevik, T., Drange, H., Jeansson, E., Li, C., Olsen, A., Skagseth, Ø., Slater, D.A., Straneo, F., Våge, K., Årthun, M., 2022. Nordic Seas Heat Loss, Atlantic Inflow, and Arctic Sea Ice Cover Over the Last Century. Rev. Geophys. 60 (1), e2020RG000725 https://doi.org/10.1029/2020RG000725.

Solomon, A., Heuzé, C., Rabe, B., Bacon, S., Bertino, L., Heimbach, P., Inoue, J., Iovino, D., Mottram, R., Zhang, X., Aksenov, Y., McAdam, R., Nguyen, A., Raj, R.P., Tang, H., 2021. Freshwater in the Arctic Ocean 2010–2019. Ocean Sci. 17 (4), 1081–1102. https://doi.org/10.5194/OS-17-1081-2021.

Stewart, K.D., Haine, T.W.N., 2016. Thermobaricity in the transition zones between alpha and beta oceans. J. Phys. Oceanogr. 46 (6), 1805–1821. https://doi.org/10.1175/JPO-D-16-0017.1.

Swift, J.H., Aagaard, K., 1981. Seasonal transitions and water mass formation in the Iceland and Greenland seas. Deep Sea Res. Part A 28 (10), 1107–1129. https://doi.org/10.1016/0198-0149(81)90050-9.

Tsubouchi, T., Våge, K., Hansen, B., Larsen, K.M.H., Østerhus, S., Johnson, C., Jónsson, S., Valdimarsson, H., 2021. Increased ocean heat transport into the Nordic Seas and Arctic Ocean over the period 1993–2016. Nat. Clim. Chang. 11 (1), 21–26. https://doi.org/10.1038/s41558-020-00941-3.

Tuerena, R.E., Hopkins, J., Buchanan, P.J., Ganeshram, R.S., Norman, L., Jvon-Appen, W., Tagliabue, A., Doncila, A., Graeve, M., Ludwichowski, K., Dodd, P.A., Vega, C., Salter, I., Mahaffey, C., 2021. An Arctic strait of two halves: the changing dynamics of nutrient uptake and limitation across the Fram Strait. Glob. Biogeochem. Cycles 35, e2021GB006961. https://doi.org/10.1029/2021GB006961.

Våge, K., Papritz, L., Håvik, L., Spall, M.A., Moore, G.W.K., 2018. Ocean convection linked to the recent ice edge retreat along east Greenland. Nat. Commun. 9 (1) https://doi.org/10.1038/S41467-018-03468-6.

von Appen, W.J., Waite, A.M., Bergmann, M., Bienhold, C., Boebel, O., Bracher, A., Cisewski, B., Hagemann, J., Hoppema, M., Iversen, M.H., Konrad, C., Krumpen, T., Lochthofen, N., Metfies, K., Niehoff, B., Nöthig, E.M., Purser, A., Salter, I., Schaber, M., Scholz, D., Soltwedel, T., Torres-Valdes, S., Wekerle, C., Wenzhöfer, F., Wietz, M., Boetius, A., 2021. Sea-ice derived meltwater stratification slows the biological carbon pump: results from continuous observations. Nat. Commun. 12 (1), 1–16. https://doi.org/10.1038/s41467-021-26943-z.

Wadhams, P., Comiso, J.C., 1999. Two modes of appearance of the Odden ice tongue in the Greenland Sea. Geophys. Res. Lett. 26 (16), 2497–2500. https://doi.org/10.1029/1999GL900502.

Walsh, J.E., Portis, D.H., 1999. Variations of precipitation and evaporation over the North Atlantic Ocean. J. Geophys. Res. Atmos. 104, 16613–16631.

Yamaguchi, R., Suga, T., 2019. Trend and variability in global upper-ocean stratification since the 1960s. J. Geophys. Res. Oceans 124 (12), 8933–8948. https://doi.org/10.1029/2019JC015439.

You, Y., 2002. A global ocean climatological atlas of the Turner angle: implications for double-diffusion and water-mass structure. Deep Sea Res. I 49 (11), 2075–2093. https://doi.org/10.1016/S0967-0637(02)00099-7.

Zuo, H., Balmaseda, M.A., Tietsche, S., Mogensen, K., Mayer, M., 2019. The ECMWF operational ensemble reanalysis-analysis system for ocean and sea ice: a description of the system and assessment. Ocean Sci. 15, 779–808. https://doi.org/10.5194/os-15-779-2019.